

# $H\beta$ Line Width and the UV-X-ray Spectra of Luminous AGN

Beverley J. Wills, Zhaohui Shang & Juntao M. Yuan

*Department of Astronomy, RLM 15.308, The University of Texas, Austin, Texas  
78712 USA*

---

## Abstract

The width of the broad  $H\beta$  emission line is the primary defining characteristic of the NLS1 class. This parameter is also an important component of Boroson and Green’s optical “Eigenvector 1” (EV1), which links steeper soft X-ray spectra with narrower  $H\beta$  emission, stronger  $H\beta$  blue wing, stronger optical Fe II emission, and weaker [O III]  $\lambda 5007$ . Potentially, EV1 represents a fundamental physical process linking the dynamics of fueling and outflow with the accretion rate. We attempted to understand these relationships by extending the optical spectra into the UV for a sample of 22 QSOs with high quality soft-X-ray spectra, and discovered a whole new set of UV relationships that suggest that high accretion rates are linked to dense gas and perhaps nuclear starbursts. While it has been argued that narrow (BLR)  $H\beta$  means low Black Hole mass in luminous NLS1s, the CIV  $\lambda 1549$  and Ly $\alpha$  emission lines are broader, perhaps the result of outflows driven by their high Eddington accretion rates. We present some new trends of optical-UV with X-ray spectral energy distributions. Steeper X-ray spectra appear associated with stronger UV relative to optical continua, but the presence of strong UV absorption lines is associated with depressed soft X-rays and redder optical-UV continua.

*Key words:* galaxies: active; quasars: general; quasars: emission lines; X-rays: galaxies

---

## 1 Introduction

The Boroson and Green (1992, BG92) “Eigenvector 1” (EV1) is one of the reasons NLS1 are interesting, and why we are having a meeting about them. EV1 (also called Principal Component 1) is a linear combination of correlated optical and X-ray properties representing the greatest variation among a set of spectra. EV1 links narrower (BLR)  $H\beta$  with stronger  $H\beta$  blue wing, stronger Fe II optical emission, and weaker [OIII]  $\lambda 5007$  emission from the NLR, with

steeper soft X-ray spectra (Laor et al. 1994, 1997). The narrower  $H\beta$  defining NLS1s has been suggested to result from lower Black Hole masses, and therefore higher accretion rates relative to the Eddington limit in these luminous AGN. The NLS1s' steep X-ray spectra are also suggested to tie in with high Eddington accretion rates (e.g. Laor, these proceedings).

In order to understand these relationships, we have extended the optical spectra of an essentially complete sample of 22 PG QSOs to UV wavelengths. The QSOs of our sample are selected (by Laor et al. 1994) to have low Galactic hydrogen absorption in order to derive reliable soft X-ray slopes and intrinsic absorption. The uncertainties in absorption correspond to less than 5% uncertainty in flux density at  $Ly\alpha$ . Five of these QSOs are NLQ1s<sup>1</sup> (with  $H\beta$  FWHMs  $< 2000 \text{ km s}^{-1}$ ): PG 1001+054 (a BAL QSO,  $1740 \text{ km s}^{-1}$ ), PG 1115+407 ( $1720 \text{ km s}^{-1}$ ), PG 1402+261 ( $1910 \text{ km s}^{-1}$ ), PG 1440+356 (Mrk 478,  $1450 \text{ km s}^{-1}$ ) and PG 1543+489 ( $1560 \text{ km s}^{-1}$ ). For comparison with X-ray selected samples, we note that the  $U - B$  color criterion for selecting the PG QSOs (Schmidt & Green 1983) is roughly equivalent to the hardness-ratio criterion ( $HR1 < 0$ ) used to select soft X-ray AGNs (e.g. Grupe et al. 1998).

We address different aspects of the Eigenvector 1 relationships: (i) The correlations among UV and optical emission lines, and soft X-ray slope. We also present the Eigenvector 1 UV-optical relationships via a spectral principal component analysis. (ii) We show relationships among line widths, and (iii) we show new relationships between the UV-optical and X-ray spectral energy distributions (SEDs). We show how the 5 NLQ1s of our sample fit into these relationships.

## 2 The UV Eigenvector 1 Relationships

Examples of our spectra, over the entire UV-optical range, presented in order of optical EV1, are shown in Fig. 1 (see also Wills et al. 1999a,b, Francis & Wills 1999). Inspection shows that, with changing EV1, in the sense of decreasing  $H\beta$  width and increasing strength of the FeII(optical) blends, the UV spectrum changes: CIV  $\lambda 1549$  is weaker and broader, Si III]  $\lambda 1892$  and nearby Fe III blends become more prominent relative to C III]  $\lambda 1909$ , and the strength of low-ionization O I  $\lambda 1304$  and C II  $\lambda 1335$  increases. Low velocity CIV gas appears to be strongly related to the optical NLR [O III]  $\lambda 5007$  emission (Brotherton & Francis 1999). Because Si III]  $\lambda 1892$  has a higher critical

---

<sup>1</sup> At optical wavelengths an observational distinction has been made between the higher luminosity QSOs ( $L > 10^{11.3} L_{\odot}$ ,  $H_0 = 100 \text{ km s}^{-1} \text{ Mpc}^{-1}$ ), where nuclear light dominates that from the host galaxy, and the lower luminosity Seyfert galaxies. We refer to QSOs with narrow BLR  $H\beta$  as NLQ1s.

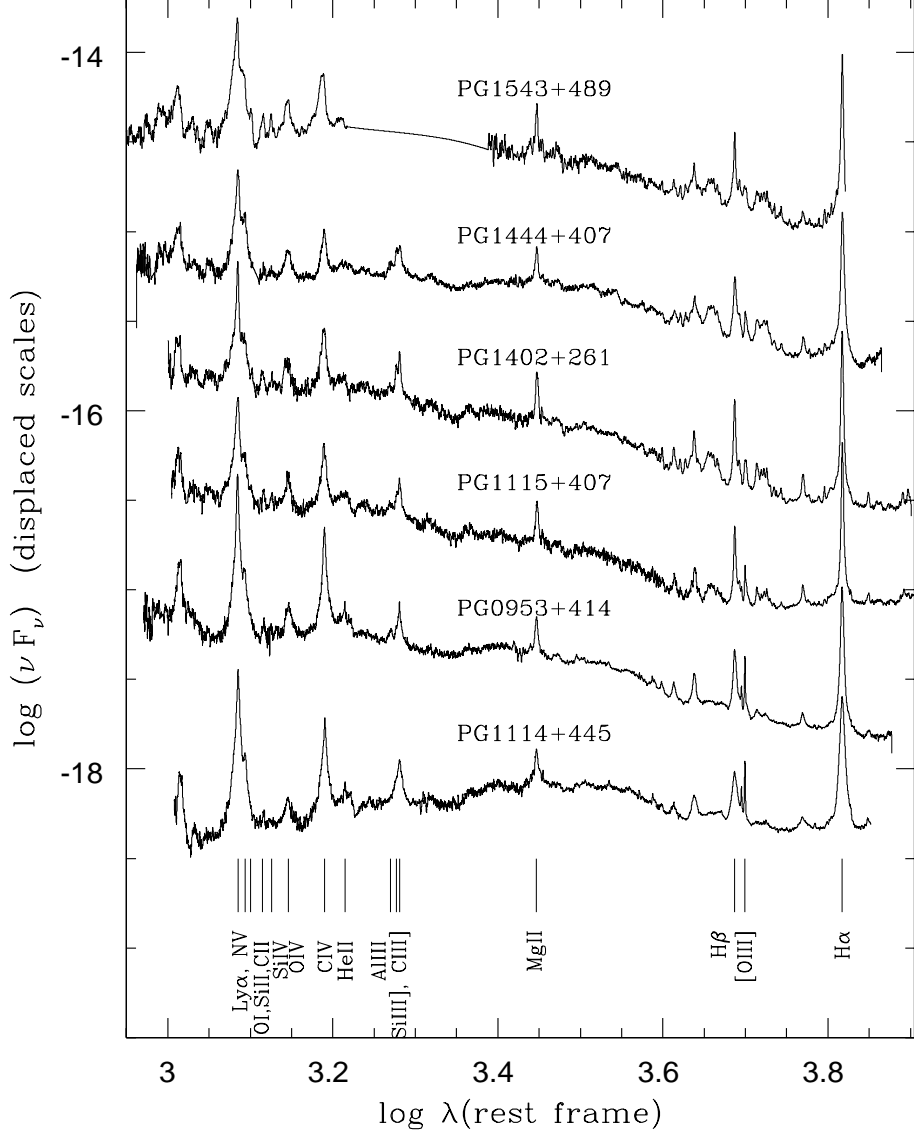


Fig. 1. Above, Hubble Space Telescope (UV, Faint Object Spectrograph) and McDonald Observatory (ground-based) spectra for several of the objects in the complete sample. These are in order of optical-X-ray Principal Component 1 (BG92, Laor et al. 1994), with the strongest Fe II(optical) and weakest [O III] NLR emission at the top.

density than the C III] transition, we surmise that increasing Fe II(optical), and narrower H $\beta$ , correspond to the increasing contribution from very dense gas,  $> 10^{10.5} \text{ cm}^{-3}$ . Unexpectedly, the high-ionization N V  $\lambda 1240$  line strength appears to increase with increasing density. We speculate that the higher-density gas is nitrogen enriched, and the copious dense gas is a result of circumnuclear starbursts. As suggested by BG92, this dense gas reduces the flux of ionizing photons reaching the more extended NLR, resulting in the inverse Fe II(optical)–[O III] relationship. In Fig. 1 the continuum of PG 1114+445 is seen to be significantly reddened; apparently dust is associated with the high-

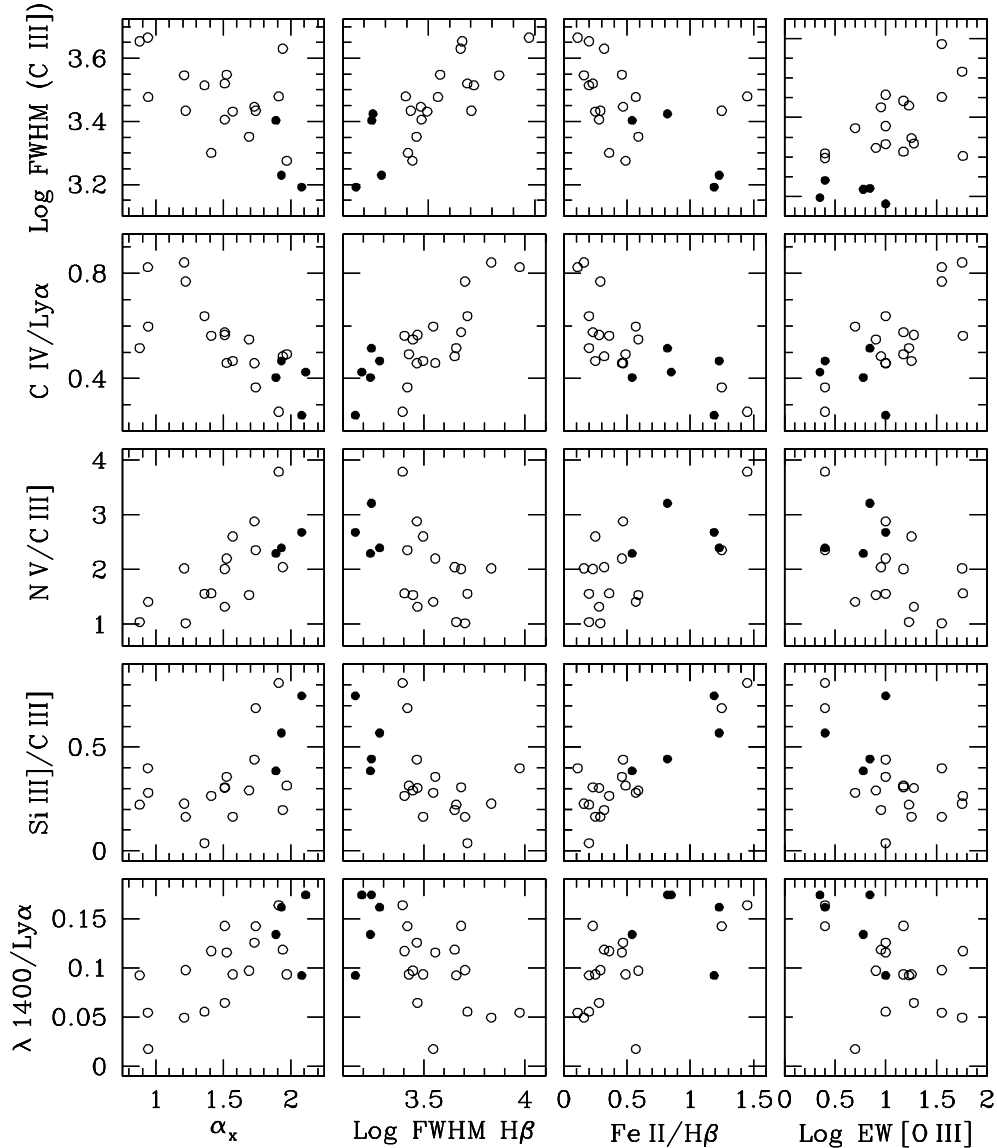


Fig. 2. Correlations corresponding to the variations illustrated in Fig. 1. New UV observables are displayed vs.  $\alpha_x$  and some optical (BG92) Principal Component 1 parameters. The two-tailed probability of these correlations arising by chance from unrelated variables is between 1 in 50 and 1 in  $\gg 1000$ .

ionization UV line absorption and the X-ray warm absorption in this QSO (George et al. 1997; Mathur et al. 1998).

Some correlations between optical EV1 parameters and new UV emission-line parameters are illustrated in Fig. 2. The NLQ1s are distinguished by filled circles. The two-tailed probability of these correlation arising from truly unrelated variables ranges from 1 in 50 to 1 in  $\gg 1000$ . Note that NLQ1s also contribute to these trends. In the UV they have weaker, broader CIV, stronger NV, stronger low-ionization lines and more dense gas (as indicated by a larger ratio, Si III]  $\lambda 1892$ /C III]  $\lambda 1909$ ). Note also that correlations with the

X-ray spectral index  $\alpha_x$  exist despite the characteristic rapid X-ray variability of the NLQ1s.

### 2.1 Spectral Principal Component Analyses

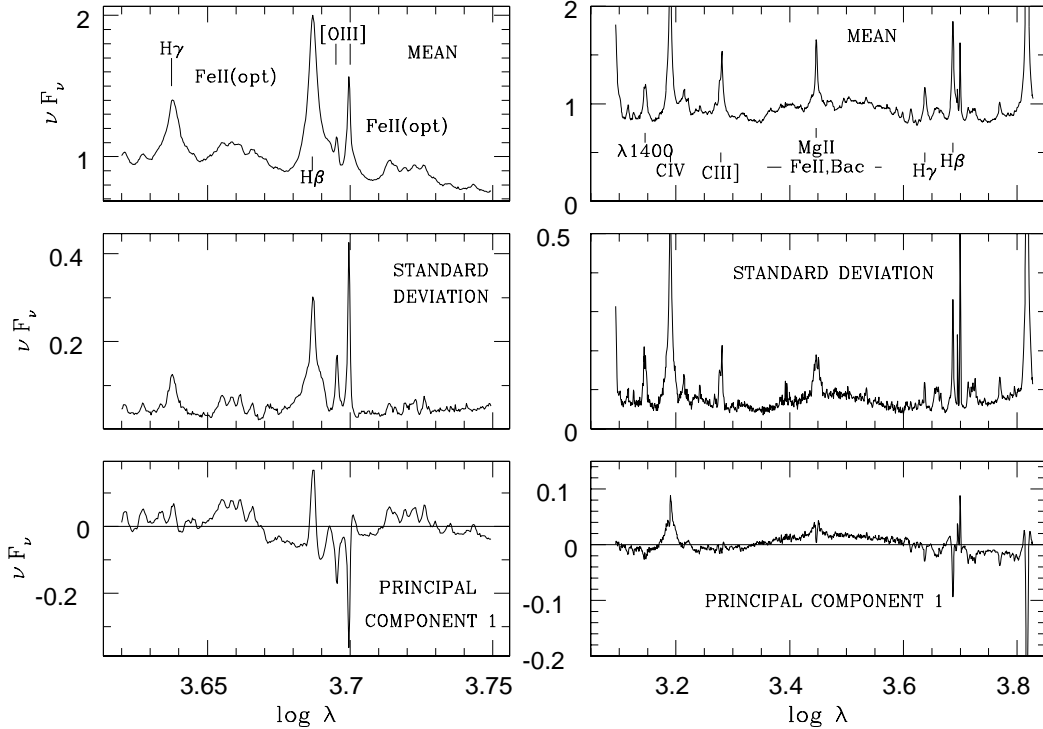


Fig. 3. The aligned mean, standard deviation and principal component 1 spectra in the H $\beta$  region (left) and the CIV  $\lambda$ 1549 – H $\alpha$  region (right). Emission from the lowest velocity gas, in the Narrow and Broad Line Regions (NLR, BLR) accounts for most of the spectrum-to-spectrum diversity.

The above trends can be illustrated in another informative way. Fig. 3 shows the mean spectrum in the H $\beta$  region (left) and in the range from CIV  $\lambda$ 1549 to H $\alpha$  (right). Ly $\alpha$  is excluded to avoid the complication of strong absorption in a few objects. A standard deviation spectrum in the middle panel shows that most of the spectrum-to-spectrum variation appears to arise from emission from low-velocity gas. This is true for Ly $\alpha$ , CIV, the Balmer lines, and Fe II(optical) blends. Because the sample is small we show only the first eigenvector, approximately equivalent to BG92’s EV1 (lower panel). Now we can see which parts of the spectrum vary together or are anticorrelated. The well-known BG92 correlation between the blended Fe II(optical) emission and the narrow BLR H $\beta$  shows clearly, as well as their anticorrelation with narrow [O III]  $\lambda$ 4959,5007. Detailed inspection of the H $\beta$  region shows that the lower-velocity gas of the Fe II(optical) emission contributes most to the correlations. (Compare the resolved peaks in the middle and lower panels with the smoother Fe II(optical) blends in the mean spectrum). The UV Fe II blends

between about 2200Å and 3600Å ( $\log \lambda$  between 3.34 and 3.56) appear anticorrelated with the strength of optical Fe II blends – probably an effect of optical depth in the optically-thick UV resonance transitions, giving rise to the lower optical depth Fe II optical transitions. This is consistent with the explanation for the weaker [O III] in objects with strong Fe II(optical) emission.

This simple interpretation is preliminary but serves to relate the significant correlations with the overall spectrum. Spectral principal component analysis is a powerful tool for analysing linear correlations. Possibly NLS1-type gas is actually present in all QSOs, but with differing contributions to the overall spectra. If so, this would represent a different point of view on the significance of NLS1 line widths. One point remains clear – the luminous NLS1s are, spectroscopically, simply more extreme than broader-line QSOs, but not fundamentally different.

### 3 Line Widths

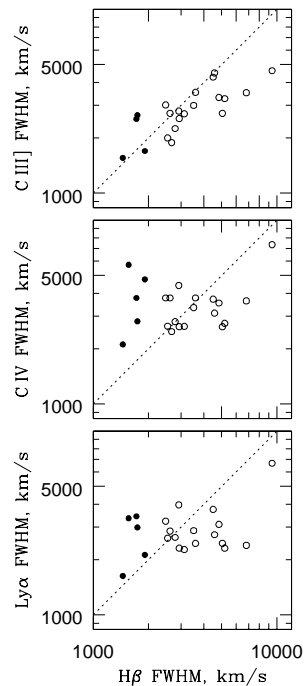


Fig. 4. Linewidth relationships. The C III]  $\lambda 1909$  line has been deblended from Si III]  $\lambda 1892$  and, where significant, from Fe III emission. The C IV FWHM is as observed, not corrected for doublet separation, which would be less than a 10% correction. Ly  $\alpha$  has been deblended from NV  $\lambda 1240$ . Note the significant ( $< 2 \times 10^{-5}$  probability of it arising by chance) correlation between FWHM of C III] and H $\beta$ , but not for C IV or Ly $\alpha$ . The dashed lines indicate equal line-width relationships.

In a sample with a wide range in luminosity, line width is seen to increase with luminosity. This leads one to question whether the defining criterion for NLS1s

or NLQ1s should be a function of luminosity! Even for our small sample the trends of FWHM with luminosity are just significant at the  $\sim 1\%$  level. The data are consistent with a (luminosity) $^{1/4}$  dependence of linewidth expected if gravity dominates the cloud motions (e.g. Laor, these proceedings). Anyway, within our sample, EV1 dominates the spectrum-to-spectrum variations.

Correlations between the widths of the UV broad lines and that of  $H\beta$  are shown in Fig. 4. The widths of C III]  $\lambda 1909$  and  $H\beta$  are strongly correlated, and similarly within the same QSO spectrum. The lower-ionization C III] emission probably arises in the same region as  $H\beta$ . It seems surprising that the widths of the hydrogen lines,  $H\beta$  and  $Ly\alpha$ , are not correlated. Neither  $Ly\alpha$  or C IV widths are correlated with C III] or  $H\beta$  widths.  $Ly\alpha$  and C IV widths are correlated with each other, however (significant at the 0.01% level, 2-tailed). We recall that the strength of the lower-velocity C IV emission is strongly correlated with the strength of [O III]  $\lambda 5007$  emission (Figs. 1–3). So part of the C IV profile becomes *narrower* as Fe II(optical) increases, or as  $H\beta$  becomes *broader*. So the lack of correlation between C IV and  $H\beta$  widths is not so surprising. This lower-velocity C IV-emitting region, called the ILR, an intermediate line region between the highest-velocity VBLR and the NLR, was related to other UV lines in high redshift QSOs by Wills et al. (1993) and Brotherton et al. (1994a,b) (see also, Brotherton & Francis 1999). The trends for high- $z$  QSOs are consistent with our present results for the low-redshift QSO sample. Note that the ‘narrow-line’ QSOs (e.g., Foltz et al. 1987, Baldwin et al. 1988) refer to the strength of the ILR in C IV – inversely related to the width of  $H\beta$  that defines the NLS1s and NLQ1s! The results of the previous section (Fig. 3) show that much of the Fe II(optical) emission has narrow widths like  $H\beta$ , consistent with both species arising in the same dense gas.

The  $H\beta$  widths have been suggested as an indicator of low Black Hole mass for NLS1s (Laor, these Proceedings). It has been suggested that  $H\beta$  and C III] might arise from an optically-thick disk, and C IV and  $Ly\alpha$  may be produced in a high-ionization wind (Murray & Chiang 1998, Bottorff et al. 1997, König & Kartje 1994). If the emission lines are produced by different kinematic gas components, then a direct kinematic interpretation of their FWHM is not reasonable. Note that the line widths for  $Ly\alpha$  and C IV are always broader than that of  $H\beta$  for the NLQ1s in our sample. This may be consistent with the suggestion that NLQ1s tend to be lower mass objects with high accretion rates that drive an outflow; the higher-ionization lines may be partly broadened by radiation-pressure driven outflow.

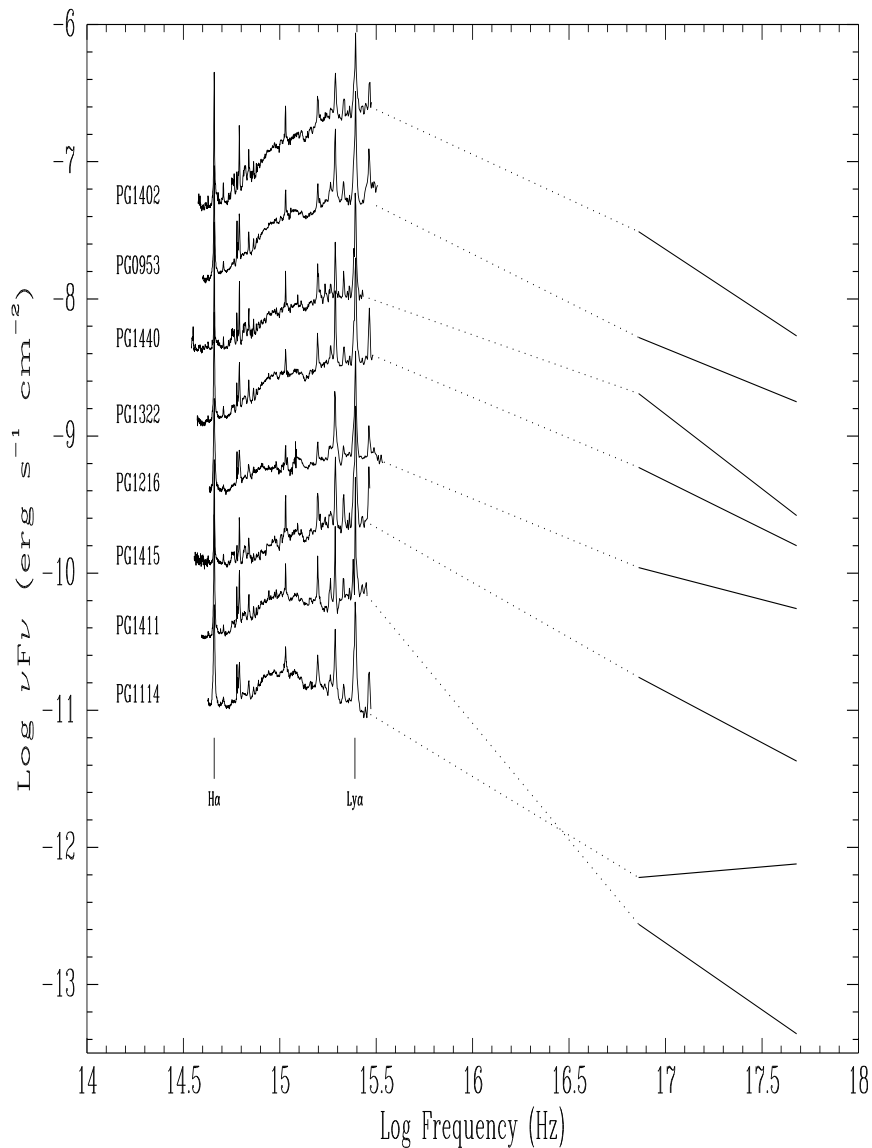


Fig. 5. Above are Spectral Energy Distributions of QSOs. The optical-UV spectra are equally displaced in  $\log \nu F_\nu$  in the continuum at  $H\alpha$ . The  $H\alpha$  and  $Ly\alpha$  emission lines are marked. The soft X-ray spectra are ROSAT data from Laor et al. (1994, 1997), and the observational uncertainties in these plots are very small on the scale of this figure. The ROSAT spectra are joined by a dotted line to the UV continuum. All spectra are corrected for absorption in our Galaxy.

#### 4 The Spectral Energy Distributions

We compare our well-calibrated HST-McDonald spectral energy distributions with the ROSAT soft X-ray spectra ( $H\alpha$  to 2 keV, Fig. 5). The spectra are separated by equal logarithmic increments in  $\nu L_\nu$  at the continuum wavelength



of  $H\alpha$ . While it is difficult to illustrate with just the few spectra of Fig. 5, we find some interesting trends in the whole sample:

- QSOs with strong UV absorption lines have redder optical-UV continua, and either weaker or flatter soft X-ray spectra. This is the case for the following QSOs of our sample: 1114+445, 1411+442, 1309+355 (radio intermediate), 1001+054 (a NLQ1), and 1425+267 (radio-loud).
- Relative to the optical-UV spectra, anchored at the  $H\alpha$  continuum, the soft X-ray spectra point towards the UV spectra – either having a steeper X-ray continuum with weaker hard X-rays, or a flatter, but stronger X-ray spectrum. This effect is significant for the whole sample at about the  $3\sigma$  level.
- The well-known trend for radio-loud QSOs to have stronger, flatter soft X-ray continua is shown clearly for PG 1226+023 (3C 273) and PG 1512+370 (4C 37.43) (not illustrated here).

The NLQ1s partake of these trends (although none in our sample is radio-loud).

## 5 Summary

The NLQ1s of our sample follow the Eigenvector 1 relationships demonstrated for the whole QSO sample in Figs. 1 and 2. Not only is this true for the  $H\beta$ –[O III] region, but it extends to the UV spectra as well. The NLQ1s therefore show narrow C III]  $\lambda$ 1909 emission lines, small ratios of CIV  $\lambda$ 1549/Ly $\alpha$ , larger ratios of NV  $\lambda$ 1240/C III]  $\lambda$ 1909, Si III]  $\lambda$ 1892/C III]  $\lambda$ 1909, and  $\lambda$ 1400/Ly $\alpha$ . These trends suggest copious amounts of high-density gas in NLQ1s, which is probably the same gas that suppresses the ionizing-photon flux available to the extended NLR. Strong nitrogen emission suggests that the gas may be enriched, perhaps by starbursts from mergers that fuel the high Eddington accretion rates in NLQ1s.

The high Eddington accretion rates may drive high-ionization outflows; this could explain the broader Ly $\alpha$  and CIV $\lambda$ 1549/Ly $\alpha$  emission lines in NLQ1s.

The soft X-ray spectra ‘point at’ the UV continuum. The steep X-ray spectra of the NLQ1s correspond to strong UV bumps in these QSOs. However, absorption apparently causes reddening of the optical-UV SEDs, strong UV line absorption, and suppression of soft X-rays.

## Acknowledgements

We thank our collaborators A. Laor, D. Wills, M. Brotherton, B. Wilkes and G. Ferland. B.J.W. is very grateful to the organizing committee, and the Wilhelm und Else Heraeus-Stiftung, for support to attend this exciting meeting. We thank the staff of McDonald Observatory, especially David Doss and Marian Frueh, also Anne Kinney, Jen Christiansen and Tony Keyes of the Space Telescope Science Institute. The research of B.J.W. has been supported by LTSA grant NAG5-3431 and grant GO-06781 from the Space Telescope Science Institute, which is operated by the Association of Universities for Research in Astronomy, Inc., under NASA contract NAS5-26555.

## References

- [1] J.A. Baldwin, R. McMahon, C. Hazard and R.E. Williams, *ApJ* **327** (1988) 103.
- [2] T.D. Boroson and R.F. Green, *ApJS* **80** (1992) 109.
- [3] M. Bottorff, K.T. Korista, I. Schlosman and R.D. Blandford, *ApJ* **479** (1997) 200.
- [4] M.S. Brotherton and P.J. Francis in: G. Ferland and J. Baldwin, eds., *Quasars and Cosmology* (Astron. Soc. of Pacific Conf. Ser 162, 1999) 395.
- [5] C.B. Foltz et al., *AJ* **94** (1987) 1423.
- [6] P.J. Francis and B.J. Wills, in: G. Ferland and J. Baldwin, eds., *Quasars and Cosmology* (Astron. Soc. of Pacific Conf. Ser 162, 1999) 363.
- [7] I.M. George et al., *ApJ* **491** (1997) 508.
- [8] D. Grupe, K. Beuermann, H.-C. Thomas, K. Mannheim and H.H. Fink, *A&A* **330** (1998) 25.
- [9] A. Königl and J.F. Kartje, *ApJ* **434** (1994) 446.
- [10] A. Laor, F. Fiore, M. Elvis, B. Wilkes and J.C. McDowell, *ApJ* **435** (1994) 611.
- [11] A. Laor, F. Fiore, M. Elvis, B. Wilkes and J.C. McDowell, *ApJ* **477** (1997) 93.
- [12] S. Mathur, B. Wilkes and M. Elvis, *ApJ* **503** (1998) 23L.
- [13] N. Murray and J. Chiang, *ApJ* **494** (1998) 125.
- [14] M. Schmidt and R.F. Green, *ApJ* **269** (1983) 352.
- [15] B.J. Wills, et al., *ApJ* **515** (1999) L53.
- [16] B.J. Wills, et al., in: G. Ferland and J. Baldwin, eds., *Quasars and Cosmology* (Astron. Soc. of Pacific Conf. Ser 162, 1999) 373.